Dynamic periodic event-triggered control for nonlinear plants with state feedback ⋆

Mani H. Dhullipalla, Hao Yu, Tongwen Chen

Department of Electrical and Computer Engineering, University of Alberta, Edmonton, AB, T6G 1H9, Canada (e-mail: dhullipa@ualberta.ca; hy10@ualberta.ca; tchen@ualberta.ca).

Abstract: In this work, we propose two methods to design a dynamic periodic event-triggered controller that stabilizes nonlinear plants using static state feedback. The design methodology begins by assuming the knowledge of a continuous-time state-feedback controller that stabilizes the nonlinear plant. Considering an event-driven controller updation, the resultant closed-loop plant is modelled as a hybrid system. Two approaches are proposed for the event-triggering mechanism (ETM) depending on continuous availability of states. Each method provides an ETM and an upper bound on the sampling period that ensures closed-loop stability. We provide some remarks comparing the two approaches and substantiate them through an illustrative example.

Keywords: Event-triggered control, nonlinear systems, state feedback, stabilization

1. INTRODUCTION

Digital implementation of control systems in a plant typically involves sampling available states or outputs and executing the computed control inputs at the actuators. Usually the sampling and execution of control tasks is periodic giving way to sampled-data control systems. A possible drawback of these systems is that periodic controllers provide needless inputs even when the performance is satisfactory. In most cases, this results in unnecessary energy consumption and actuator wear. Compared to the traditional approach, event-triggered control (ETC) has been shown to significantly reduce the number of samplings (and controller updates) in Nesic et al. [2009], Mazo et al. [2010] and the references therein. Central to ETC, however, is the design of ETM that makes decisions on signal transmission and controller updation. Usually ETM is evaluated continuously which leads to usage of more energy resources than intended defeating the primary motive of ETC. To overcome the necessity of continuous monitoring, in recent years a new approach termed periodic event-triggered control (PETC) has been proposed where the ETM is evaluated periodically, see Heemels et al. [2015].

PETC for linear plants has been studied via three approaches, namely: 1) impulsive system approach; 2) perturbed linear system approach; and 3) piecewise linear system approach, see Heemels et al. [2013]. However, in this work we are interested in nonlinear systems and as mentioned in Heemels et al. [2015], several stability results obtained for linear plants are difficult to generalize to nonlinear plants. Instead, emulation-based approaches are pursued to build PETC schemes for nonlinear plants with a focus on designing the sampling period and the ETM.

One way to construct a PETC scheme is to start from an existing continuous-time event-triggered controller that stabilizes the nonlinear plant, see Postoyan et al. [2013]. The discussion in this case is focused on re-designing the ETM and systematically designing the sampling period, or its bounds, that ensures stability. Alternatively relaxing the assumption on existence of a continuous-time event-triggered controller, Wang et al. [2016] started with an existing continuous-time state feedback controller and focused on designing ETM. In this method, the design of sampling periods was a consequence of the hybrid systems approach adopted.

Contrary to Postoyan et al. [2013] and Wang et al. [2016], this work proposes two methodologies to construct dynamic PETC schemes for stabilizing nonlinear plants with state feedback. Dynamic event-triggered control, introduced in Girard [2015], has been shown to have potential in significantly reducing the number of events triggered for the same level of performance compared to static ETC, see Borgers et al. [2016], Dolk et al. [2017], Yu et al. [2019]. Dynamic PETC for linear systems was first discussed in Borgers et al. [2017]. To the best of our knowledge, dynamic PETC scheme for nonlinear systems has not been investigated yet.

The two methods proposed in this paper differ in the construction of dynamic ETM; one requires continuous availability of states of the plant and the other relaxes this assumption. We start by assuming the knowledge of an existing static state-feedback controller that stabilizes the nonlinear plant. Subsequently, we define auxilliary variables that facilitate the formulation of dynamic ETM evaluated at specific sampling instants (event-verifying instants). The dynamic ETM and an upper bound on the sampling period, called maximum allowable sampling period (MASP), is obtained as a consequence of stability analysis.

This paper is organized as follows. Section 2 introduces some standard notations and specific definitions used in the paper. The description and formulation of the problem is addressed in Section 3. Section 4 discusses two methods of dynamic PETC schemes providing stability analysis in each case. An illustrative example discussing the two methods is provided in Section 5 followed by conclusive remarks in Section 6.

2. PRELIMINARIES

Denote $\mathbb{R}$ to be set of real numbers, $\mathbb{Z}$ to be the set of integers then $\mathbb{R}_{\geq 0} = [0, \infty)$ and $\mathbb{Z}_{\geq 0} = \{0, 1, 2, \dots\}$. Let $|x|$ be the Euclidean norm of an n-dimensional vector $x \in \mathbb{R}^n$. A continuous function $\alpha : [0, a) \to \mathbb{R}_{\geq 0}$ is said to be of class $\mathcal{K}$ if it is strictly increasing and $\alpha(0) = 0$. Further, α is said to be of class $\mathcal{K}_\infty$ if $\alpha(r) \to \infty$ as $r \to \infty$. A continuous function $\beta : [0, a) \times \mathbb{R}_{\geq 0} \to \mathbb{R}_{\geq 0}$ is said to be of class $\mathcal{KL}$ if for a fixed $r \in \mathbb{R}_{\geq 0}$, $\beta(\cdot, r)$ belongs to class $\mathcal{K}$ and for a fixed $s \in [0, a)$, $\beta(s, \cdot)$ decreases to zero. The Clarke derivative, in Clarke [1983], is defined as follows: for a locally Lipschitz function $U : \mathbb{R}^n \to \mathbb{R}$ and a vector $v \in \mathbb{R}^n$, $U^\circ(x, v) := \limsup_{h \to 0^+, y \to x} \frac{U(y+hv) - U(y)}{h}$. For a C^1 function $U(\cdot)$, the Clarke derivative $U^\circ(x, v)$ reduces to the standard directional derivative $\langle \nabla U(x), v \rangle$, where $\langle \cdot, \cdot \rangle$ is the inner product and $\nabla U(\cdot)$ is the classical gradient. This definition is useful to treat locally Lipschitz functions which are not differentiable everywhere, specifically applicable for Lyapunov functions defined in our study.

The following lemma is used to show asymptotic stability via Lyapunov analysis that is discussed in Section 4.

Lemma 1. (Clarke [1983], Liberzon et al. [2014]). Consider two functions $U_1 : \mathbb{R}^n \to \mathbb{R}$ and $U_2 : \mathbb{R}^n \to \mathbb{R}$ that have well-defined Clarke derivatives for $x \in \mathbb{R}^n$ and $v \in \mathbb{R}^n$. Introduce three sets $\mathcal{A} := \{x : U_1(x) > U_2(x)\}, \mathcal{B} := \{x : U_1(x) < U_2(x)\}, \Omega := \{x : U_1(x) = U_2(x)\}$. Then for any $v \in \mathbb{R}^n$, the function $U(x) := \max\{U_1(x), U_2(x)\}$ satisfies $U^\circ(x; v) = U_1^\circ(x; v)$ for $x \in \mathcal{A}$, $U^\circ(x; v) = U_2^\circ(x; v)$ for $x \in \mathcal{B}$, and $U^\circ(x; v) \leq \max\{U_1^\circ(x; v), U_2^\circ(x; v)\}$ for $x \in \Omega$.

3. PROBLEM FORMULATION

Consider the following nonlinear plant model
$$\dot{x} = f(x, u), \qquad (1)$$
where $x \in \mathbb{R}^n$ is the state and $u \in \mathbb{R}^m$ is the control input. The function $f : \mathbb{R}^n \times \mathbb{R}^m \to \mathbb{R}^n$ is assumed to be locally Lipschitz continuous. It is assumed that the full state vector x is measured, and thus there exists a static state-feedback controller stabilizing the origin of (1):
$$u = \kappa(x), \qquad (2)$$
where $\kappa : \mathbb{R}^m \to \mathbb{R}^n$ is the controller gain function.

Due to the limited communication resources, we implement the controller in (2) in a periodic event-triggered manner. Define a time sequence $\{s_i\}_{i=0}^\infty$ that is used to check event occurrence such that
$$\varepsilon \leq s_{i+1} - s_i \leq T, \qquad (3)$$
for all $i \in \mathbb{Z}_{\geq 0}$. The upper bound $T > 0$ is to be designed, and the minimum time $\varepsilon \in (0, T]$ between the two consecutive event-verifying instants, s_i and s_{i+1}, is decided by the hardware constraints. Further, let $\{t_k\}_{k=0}^\infty \subset \{s_i\}_{i=0}^\infty$

be a subsequence denoting the triggering instants whose construction is discussed shortly.

When an event occurs at time t_k according to some designed event-triggering condition, the state $x(t_k)$ will be broadcasted to the controller node that updates the control signal. Denote $\hat{x}(t) := x(t_k)$, $t \in [t_k, t_{k+1})$, as the latest broadcasted state. The periodic event-triggered state-feedback controller is then given by
$$u = \kappa(\hat{x}). \qquad (4)$$

In this work, we will implement a dynamic periodic event-triggering condition, which involves the following piecewise continuous auxiliary variable $\eta \in \mathbb{R}_{\geq 0}$ governed by
$$
\begin{cases}
\dot{\eta} = f_c(\eta, x, e), & t \in [s_i, s_{i+1}); \\
\eta(t^+) = g_s(\eta, x, e), & t \in \{s_i\} \setminus \{t_k\}; \\
\eta(t^+) = g_t(\eta, x, e), & t \in \{t_k\};
\end{cases} \qquad (5)
$$
where $e = \hat{x} - x$ is the transmission error with $e(t_k) = 0, k \in \mathbb{Z}_{\geq 0}$ upon event occurrence. The functions $f_c, g_s, g_t : \mathbb{R}_{\geq 0} \times \mathbb{R}^n \times \mathbb{R}^n \to \mathbb{R}$ are to be designed with $f_c(0, x, e) \geq 0$ for all $x, e \in \mathbb{R}^n$. The considered dynamic ETM, evaluated at s_i, is a condition in the following form:
$$t_{k+1} = \min\{t > t_k \mid t \in \{s_i\}_{i=0}^\infty, \ g_s(\eta, x, e) < 0\} \qquad (6)$$
which results in the generation of subsequence $\{t_k\}_{k=0}^\infty$. The schematic in Fig. 1 depicts the two sequences. Without loss of generality, we assume that the event is triggered at the initial instant, i.e., $e(0) = 0$ and $t_0 = s_0 = 0$.

Let $\tau \in \mathbb{R}_{\geq 0}$ keep track of the time elapsed since the last event-verifying instant with the dynamics:
$$
\begin{cases}
\dot{\tau} = 1, & \text{when } \tau \in [0, T]; \\
\tau^+ = 0, & \text{when } \tau \in [\varepsilon, T].
\end{cases}
$$
We thus model the complete system as the following hybrid system model:
$$
\begin{aligned}
\text{flow map: } & \dot{q} = F(q), \quad q \in C; \\
\text{jump map: } & q^+ \in G(q), \quad q \in D,
\end{aligned} \qquad (7)
$$
where the augmented state $q := (x, e, \tau, \eta)$, the sets
$$
\begin{aligned}
C &:= \{q \in \mathbb{R}^{2n+2} \mid \tau \in [0, T], \ \eta \in \mathbb{R}_{\geq 0}\}; \\
D &:= \{q \in \mathbb{R}^{2n+2} \mid \tau \in [\varepsilon, T], \ \eta \in \mathbb{R}_{\geq 0}\}, \qquad (8)
\end{aligned}
$$
and the functions
$$
F(q) = \begin{bmatrix} f(x, \kappa(x+e)) \\ -f(x, \kappa(x+e)) \\ 1 \\ f_c(\eta, x, e) \end{bmatrix},
$$
$$
G(q) = \begin{cases}
\begin{bmatrix} x \\ 0 \\ 0 \\ g_t(\eta, x, e) \end{bmatrix}, & g_s(\cdot) < 0; \\[2em]
\begin{bmatrix} x \\ e \\ 0 \\ g_s(\eta, x, e) \end{bmatrix}, & g_s(\cdot) > 0; \\[2em]
\left\{ \begin{bmatrix} x \\ 0 \\ 0 \\ g_t(\eta, x, e) \end{bmatrix}, \begin{bmatrix} x \\ e \\ 0 \\ g_s(\eta, x, e) \end{bmatrix} \right\}, & g_s(\cdot) = 0.
\end{cases} \qquad (9)
$$
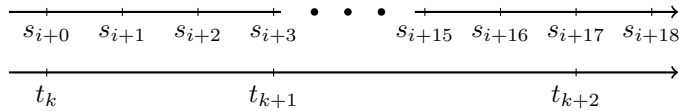
Fig. 1. Sequence of event-verifying instants s_i and triggering instants t_k.

Here, the flow set C is such that the system flows between any two event-verifying instants, say $[s_i, s_{i+1}]$, and jumps at the event-verifying instants, i.e., at both $\{s_i, s_{i+1}\}$. It is important to note that the flow map $F(q)$ and the jump map $G(q)$ in (9), are continuous and outer semi-continuous respectively. This construction in addition to C and D being closed subsets ensures nominal well-posedness of the hybrid model in (7), see Goebel et al. [2012].

The main objective of this work is to design the upper bound T and functions f_c, g_s, g_t in (5) such that the closed-loop system in (7) is asymptotically stable, that is, there exists a $\mathcal{KL}$-class function β such that for any initial state $x(0,0)$,
$$\|\varphi(t,j)\| \le \beta(\|x(0,0)\|, t+j),$$
for all $t \in \mathbb{R}_{\ge 0}$ and $j \in \mathbb{Z}_{\ge 0}$ with $\varphi := (x, e)$.

4. MAIN RESULTS

In this section, we will provide two kinds of dynamic periodic event-triggering conditions based on different assumptions on the system. In the first one, the ETM is supposed to read the state continuously (while the event is still checked for at discrete event-verifying instants, s_i). For the second kind, an ISS-Lyapunov function with a linear decay rate will be used explicitly in the event-triggering condition.

4.1 Method I

To design the upper bound T and dynamics of η, we start by introducing two assumptions, similar to those in Wang et al. [2016], made on the hybrid system in (7).
Assumption 1: For the closed-loop system in (7), there exist locally Lipschitz functions $W : \mathbb{R}^n \to \mathbb{R}_{\ge 0}$ and $V : \mathbb{R}^n \to \mathbb{R}_{\ge 0}$, $\underline{\alpha}_W, \bar{\alpha}_W, \underline{\alpha}_V, \bar{\alpha}_V, \alpha_V \in \mathcal{K}_\infty$, a continuous function $H : \mathbb{R} \to \mathbb{R}_{\ge 0}$, and constant $L, \gamma > 0$ such that the following holds:

(1) For any $e \in \mathbb{R}^n$, $\underline{\alpha}_W(\|e\|) \le W(e) \le \bar{\alpha}_W(\|e\|)$;
(2) For any $x \in \mathbb{R}^n$ and almost all $e \in \mathbb{R}^n$,
$$\langle \nabla W(e), -f(x, \kappa(x+e)) \rangle \le LW(e) + H(x);$$
(3) For any $x \in \mathbb{R}^n$, $\underline{\alpha}_V(\|x\|) \le V(x) \le \bar{\alpha}_V(\|x\|)$;
(4) For almost all $x \in \mathbb{R}^n$ and any $e \in \mathbb{R}^n$,
$$\langle \nabla V(x), f(x, \kappa(x+e)) \rangle \le -\alpha_V(\|x\|) + \gamma^2 W^2(\|e\|) - H^2(x).$$

Assumption 2: There exists a constant $l_\alpha > 0$ such that $\bar{\alpha}_V(\|s\|) \le l_\alpha H^2(s)$ for all $s \in \mathbb{R}^n$.

Items (3) and (4) in Assumption 1 imply that the system $\dot{x} = f(x, \kappa(x+e))$ is input-to-state stable (ISS) with respect to $W(e)$, and $V(x)$ is the corresponding ISS-Lyapunov function.

Subsequently, to design the upper bound T, we introduce the following concept of maximum allowable sampling period (MASP). For a given $\lambda \in (0,1)$, define $T_0(\lambda)$ as

$$T_0(\lambda) = \begin{cases} \dfrac{1}{L_\mu r} \arctan \dfrac{r(1-\lambda)}{\frac{2\gamma\lambda}{L_\mu(1+\lambda)} + \frac{\lambda^2+1}{\lambda+1}} & \gamma > L_\mu \\[4mm] \dfrac{1-\lambda}{L_\mu(1+\lambda)} & \gamma = L_\mu \quad (10) \\[4mm] \dfrac{1}{L_\mu r} \text{arctanh} \dfrac{r(1-\lambda)}{2\frac{\gamma\lambda}{L_\mu(1+\lambda)} + \frac{\lambda^2+1}{\lambda+1}} & \gamma < L_\mu, \end{cases}$$

where $r := \sqrt{\left|\left(\frac{\gamma}{L_\mu}\right)^2 - 1\right|}$ and $L_\mu := L + \mu$ with a sufficiently small constant $\mu > 0$. When λ and μ go to zero, $T_0(\lambda)$ would become the MASP, see Nesic et al. [2009]. By choosing an appropriate value for the design parameter λ, the upper bound $T = T_0(\lambda)$ is determined. Furthermore, we have the following lemma of $T_0(\lambda)$.

Lemma 2. (Nesic et al. [2009]). Let $\theta : \mathbb{R}_{\ge 0} \to \mathbb{R}$ be the solution to
$$\dot{\theta}(s) = \begin{cases} -2L_\mu\theta(s) - \gamma(\theta^2(s)+1), & s \in [0, T_0(\lambda)]; \\ 0, & s > T_0(\lambda), \end{cases}$$
with $\theta(0) = \frac{1}{\lambda}$. Then $\theta(s)$ is monotonically decreasing and $\theta(s) = \lambda$ for $s \ge T_0(\lambda)$.

The following theorem provides a method to design the event-triggering condition in (5-6).
Theorem 3. Under Assumptions 1-2, if the functions in (5) are given as
$$\begin{aligned} f_c(\eta, x, e) =& -\beta_c \eta + \sigma \alpha_V(\|x\|), \\ g_s(\eta, x, e) =& \eta + \max\{\rho V(x), \gamma\lambda W^2(e)\} \\ & - \max\{\rho V(x), \tfrac{1}{\lambda}\gamma W^2(e)\}, \\ g_t(\eta, x, e) =& \eta + \max\{\rho V(x), \gamma\lambda W^2(e)\} - \rho V(x), \end{aligned} \quad (11)$$
where $\beta_c > 0$, $\sigma \in (0,1)$, and ρ satisfies $\rho\gamma l_\alpha \le \lambda$, then the closed-loop system in (7) is asymptotically stable.

Proof. Consider the following Lyapunov function
$$U(q) = V(x) + \max\{\gamma\theta(\tau)W^2(e), \rho V(x)\} + \eta, \quad (12)$$
where $\theta(\cdot)$ is defined in Lemma 2. We start by considering stability properties on the flow set, i.e., between two event-verifying instants, and divide the analysis into three sub-cases depending on the resultant Lyapunov function $U(q)$.

Case I: When $\rho V(x) > \gamma\theta W^2(e)$, one has
$$\gamma^2 W^2(e) < \frac{\gamma\rho V(x)}{\theta} \le \frac{\gamma\rho V(x)}{\lambda} \le \frac{V(x)}{l_\alpha},$$
which leads to
$$\begin{aligned} U^\circ =& \dot{V} + \rho\dot{V} + f_c(\eta, x, e) \\ \le& (1+\rho)\left(-\alpha_V(\|x\|) + \frac{V(x)}{l_\alpha} - H^2(x)\right) + f_c(\eta, x, e) \\ \le& -(1+\rho-\sigma)\alpha_V(\|x\|) - \beta_c\eta, \end{aligned} \quad (13)$$
where the first inequality uses Assumptions 1 and 2.

Case II: When $\rho V(x) < \gamma\theta W^2(e)$ then
$$\begin{aligned} U^\circ =& \dot{V} + 2\gamma\theta W(e)\dot{W}(e) + \gamma\dot{\theta}W^2(e) + f_c(\eta, x, e) \\ \le& -\alpha_V(\|x\|) + \gamma^2 W^2(e) - H^2(x) + f_c(\eta, x, e) \\ & + 2\gamma\theta W(e)(LW(e) + H(x)) \\ & - \gamma W^2(e)[2L_\mu\theta + \gamma(\theta^2+1)] \\ \le& -2\mu\lambda\gamma W^2(e) - (1-\sigma)\alpha_V(\|x\|) - \beta_c\eta. \end{aligned} \quad (14)$$

Case III: Finally, if $\rho V(x) = \gamma\theta W^2(e)$ then from Lemma 1 it follows

$$U^\circ \leq \max\{-\rho\alpha_V(\|x\|), -2\mu\lambda\gamma W^2(e)\} \\ - (1-\sigma)\alpha_V(\|x\|) - \beta_c\eta \quad (15)$$

Then based on the definition of U and Lemma 1, (13-14) imply that there exists a positive function $\Gamma : \mathbb{R} \to \mathbb{R}_{\geq 0}$ such that

$$\langle \nabla U(q), F(q) \rangle \leq -\Gamma(U(q)), q \in C, \quad (16)$$

where $\Gamma(s)$ is decided by $\rho\alpha_V(s), \beta_c s$ and $\max\{2\mu\lambda\gamma s, (1-\sigma)\alpha_V(s)\}$.

Next, we examine stability of the system on jump sets, i.e., at event-verifying instants. The analysis here is divided into two cases depending on the triggering of an event which is decided by the sign of $g_s(\eta, x, e)$, as defined in (9).

Case I: When $g_s(\eta, x, e) \geq 0$, we have

$$U(G(q)) - U(q) = V(x) + \max\{\rho V(x), \gamma\frac{1}{\lambda}W^2(e)\} \\ - V(x) - \max\{\rho V(x), \gamma\theta W^2(e)\} \\ + g_s(\eta, x, e) - \eta \\ = \max\{\rho V(x), \gamma\lambda W^2(e)\} \\ - \max\{\rho V(x), \gamma\theta W^2(e)\} \\ \leq 0, \quad (17)$$

where the last inequality is due to $\theta(\tau) \geq \lambda$ when $\tau \leq T_0(\lambda)$.

Case II: When $g_s(\eta, x, e) < 0$, then we have

$$U(G(q)) - U(q) = (1+\rho)V(x) + g_t(\eta, x, e) - V(x) \\ - \max\{\rho V(x), \gamma\theta W^2(e)\} - \eta \quad (18) \\ \leq 0.$$

Combining (17-18) leads to

$$U(G(q)) - U(q) \leq 0, \quad (19)$$

for all $q \in D$. Therefore, the proof is completed following a similar line in Nesic et al. [2009] based on (16) and (19).

□

Remark 1: A static version of the triggering condition in Theorem 3 can be given as

$$t_{k+1} = \min\{t \in \{s_i\}, t > t_k | \gamma W^2(e) > \lambda\rho V(x)\}, \quad (20)$$

which has the similar form of that in Wang et al. [2016]. By selecting $\rho = \frac{\lambda}{\gamma l_\alpha}$, one can see that there is a tradeoff between the event-verifying periods and the inter-event steps (the number of verifying instants between two consecutive events), that is, a smaller λ would increase $T_0(\lambda)$ but would make it easier for the triggering condition (in Theorem 3 or (20)) to be satisfied.

Remark 2: By introducing the nonnegative variable η, the dynamic triggering condition in Theorem 3 can discard some transmissions even when $\gamma W^2(e) > \lambda\rho V(x)$. Thus, the capacity of dynamic triggering condition to increase η plays a key role in prolonging the inter-event times. From (11), $f_c(\eta, x, e)$ can provide some increment when x is large, while $g_t(\eta, x, e)$ deals with the case of large e. Note that η cannot increase by the jump with $g_s(\eta, x, e)$.

The main drawback of (11) is requiring the event trigger to continuously read the state measurement and conducting the integral operation. A direct solution is to modify $f_c(\eta, x, e)$ as

$$f_c(\eta, x, e) = -\beta_c\eta. \quad (21)$$

However, such an f_c would impair the capacity to increase η. The main problem of Method I is that the x-related part of U in (12) cannot offer any decrease when the system jumps. Thus, to solve this problem, some new Lyapunov function should be applied.

4.2 Method II

In this subsection, we will provide another method to design the dynamic triggering condition which only needs to read the state x at the discrete event-verifying instants. To this end, we revise Assumption 1 into the following form.

Assumption 3: Suppose that Assumption 1 holds with $\alpha_V(\|x\|) = \alpha_v V(x)$.

Assumption 3 means that the Lyapunov function V converges exponentially in the absence of measurement error e. Then based on this assumption, we introduce the following theorem.

Theorem 4. Under Assumptions 2-3, if the functions in (5) are given as

$$f_c(\eta, x, e) = -\beta_c\eta, \\ g_s(\eta, x, e) = \eta + \max\{e^{a\tau}\rho V(x), \gamma\lambda W^2(e)\} \\ - \max\{\rho V(x), \frac{1}{\lambda}\gamma W^2(e)\}, \\ g_t(\eta, x, e) = \eta + \max\{e^{a\tau}\rho V(x), \gamma\lambda W^2(e)\} - \rho V(x), \quad (22)$$

where $\beta_c > 0$ and design parameters ρ, a, b satisfy

$$a = \frac{\alpha_v\gamma l_\alpha}{\lambda}, \quad b = e^{aT_0}, \quad \rho = \frac{\lambda}{\gamma l_\alpha b}, \quad (23)$$

then the closed-loop system in (7) is asymptotically stable.

Proof. Consider the following Lyapunov function:

$$O(q) = V(x) + \max\{\gamma\theta(\tau)W^2(e), e^{a\tau}\rho V(x)\} + \eta, \quad (24)$$

where $\theta(\tau)$ is governed by Lemma 2. Similar to the analysis in Method I, we first study the behavior of O between two consecutive event-verifying instants.

Case I: When $e^{a\tau}\rho V(x) > \gamma\theta W^2(2)$, it follows that

$$\gamma^2 W^2(e) < \frac{e^{a\tau}\gamma\rho V(x)}{\theta} \leq \frac{e^{a\tau}V(x)}{l_\alpha b}$$

where $b = \frac{\lambda}{\gamma l_\alpha \rho}$. Furthermore, we have

$$O^\circ = \dot{V} + ae^{a\tau}\rho V + e^{a\tau}\rho\dot{V} + f_c(\eta, x, e) \\ \leq -\alpha_v V(x) + \gamma^2 W^2(e) - H^2(x) + ae^{a\tau}\rho V - \beta_c\eta \\ + e^{a\tau}\rho(-\alpha_v V(x) + \gamma^2 W^2(e) - H^2(x)). \quad (25)$$

According to (23), a is designed so that $\alpha_v \geq ae^{a\tau}\rho$ and $e^{a\tau} \leq b$ since $\tau \leq T_0(\lambda)$. Then, (25) implies

$$O^\circ = -\alpha_v\rho e^{a\tau}V(x) + (1 + e^{a\tau}\rho)(\gamma^2 W^2(e) - H^2(x)) \\ - \beta_c\eta \\ \leq -\alpha_v\rho e^{a\tau}V(x) - \beta_c\eta + (1 + e^{a\tau}\rho)(\frac{e^{a\tau}}{b} - 1)H^2(x) \\ \leq -\alpha_v\rho e^{a\tau}V(x) - \beta_c\eta. \quad (26)$$

Case II: When $e^{a\tau}\rho V(x) < \gamma\theta W^2(2)$, the derivation is similar to (14) and results in

$$O^{\circ} \leq -2\mu\lambda\gamma W^2(e) - \alpha_v V(x) - \beta_c\eta. \qquad (27)$$

Case III: When $e^{a\tau}\rho V(x) = \gamma\theta W^2(2)$ from Lemma 1 it follows

$$O^{\circ} \leq \max\{-\alpha_v\rho e^{a\tau}V(x), -2\mu\lambda\gamma W^2(e) - \alpha_v V(x)\} \\ - \beta_c\eta. \qquad (28)$$

Next, consider analysis at jumps that occur at event-verifying instants. Again, similar to Method I, we have the following two cases depending on event occurrence.

Case I: When $g_s(\eta, x, e) \geq 0$, we have

$$\begin{aligned} O(G(q)) - O(q) =& V(x) + \max\{\rho V(x), \gamma\frac{1}{\lambda}W^2(e)\} \\ & - V(x) - \max\{e^{a\tau}\rho V(x), \gamma\theta W^2(e)\} \\ & + g_s(\eta, x, e) - \eta \\ \leq & 0. \end{aligned} \qquad (29)$$

Case II: When $g_s(\eta, x, e) < 0$, it follows that

$$\begin{aligned} O(G(q)) - O(q) =& (1+\rho)V(x) + g_t(\eta, x, e) - V(x) \\ & - \max\{e^{a\tau}\rho V(x), \gamma\theta W^2(e)\} - \eta \quad (30) \\ \leq & 0. \end{aligned}$$

Therefore, the proof is completed by combining (26-30).

□

Remark 3: To implement the dynamic triggering condition in Theorem 4, at each event-verifying instant $s_i, i \in \mathbb{Z}_{\geq 1}$, the event trigger needs to record the time $s_i - s_{i-1}$ and calculate $e^{a(s_i - s_{i-1})}$. In the special case that the event is detected periodically, both of them are constants that can be determined offline.

Remark 4: Compared to Theorem 3, the method in this subsection can provide some extra capacity to increase η at the jump. Before the static condition $\gamma W^2(e) > \lambda\rho V(x)$ is violated, both $g_s(\eta, x, e)$ and $g_t(\eta, x, e)$ must enlarge the value of η. This feature assists in improving the inter-event time and avoids continuous reading of state measurements between two successive event-verifying instants.

Remark 5: The main drawback of Method II is using the linear decay rate α_v and its corresponding ISS-Lyapunov function explicitly. Although Praly and Wang [1996] showed that it is not restrictive to modify the ISS-Lyapunov function in Assumption 1 to satisfy Assumption 3, note that if the ISS-Lyapunov function V for Method II is derived by relaxing $H(x)$ used in Assumption 1 for Method I then this directly affects the gain γ associated with the error e. This increased γ shrinks ρ in (23) and so the event-triggering condition is easily violated compared to that of Method I. This is demonstrated by the difference in average numbers of triggers between Table 1 and Table 2 in the numerical example in Section 5.

Remark 6: If the plant in (1) is linear, then Assumption 3 is not necessary, since it is trivial to find a quadratic ISS-Lyapunov function with a linear decay rate in Assumption 1. In this case, Method II would generate less events than Method I with f_c in (21). Thus, one may prefer to use Method II when the nonlinearity of the plant is weak and no state information is available to the ETM continuously.

5. SIMULATIONS

As an illustrative example, the following locally Lipschitz nonlinear plant is considered

$$\dot{x} = -x^3 + 0.5x^2 + u, \; u = -2x. \qquad (31)$$

The corresponding event-triggered controller takes the form $u = -2\hat{x}$. For the plant in (31), the corresponding Lyapunov functions and relevant quantities for each method are as follows:

Method I (M.I): Assumption 1 is satisfied with Lyapunov functions $V = \frac{x^4}{2} + 2x^2$ and $W = |e|$, and quantities $H(x) = |x^3 - 0.5x^2 + 2x|$, $L = 2$, $\alpha_v(\|x\|) = 0.047x^6 - 0.061x^4 + 0.1892x^2$, $\gamma = 2.049$. Assumption 2 is satisfied by choosing $l_\alpha = 1$. The ETM evaluates the sign of

$$\begin{aligned} g_s(\eta, x, e) =& \eta + \max\{0.34V(x), 1.73e^2\} \\ & - \max\{0.34V(x), 2.62e^2\}. \end{aligned} \qquad (32)$$

Method II (M.II): In order to satisfy Assumption 3, $H(x)$ in Assumption 1 is considered to be of the form $H(x) = |px^3 - 0.5x^2 + rx|$, $p > 1, r > 2$. The resultant Lyapunov function satisfying the assumption is $V = \frac{px^4}{2} + rx^2$ with $p = 1.97$, $r = 3.87$ and α_v is 0.08. Additionally for Assumption 1, we also have $W = |e|$, $L = 2$, and $\gamma = 26.79$. l_α in Assumption 2 is chosen to be 1. The ETM that evaluates the sign of $g_s(\eta, x, e)$, given by

$$\begin{aligned} g_s(\eta, x, e) =& \eta + \max\{0.003V(x), 2.12e^2\} \\ & - \max\{7.7 \cdot 10^{-4}V(x), 337.3e^2\}. \end{aligned} \qquad (33)$$

In Fig. 2(a), the upper bound $T = T_0(\lambda)$ is plotted as a function of design parameter λ for each method. Stabilization of the plant using both methods is depicted through the state trajectories in Fig. 2(b). As stated in Remark 5 of Section 4, the increase in γ directly affects the performance (namely, the average number of triggers) of the method, as seen in (32), (33). Notice that the gain γ in M.II is substantially higher than that in M.I and the difference in no. of triggers of M.I in Table 1 and those of M.II in Table 2 demonstrate its effect. Further, we compare M.I and its variant M.I ($\sigma = 0$) with those of Wang et al. [2016] and Postoyan et al. [2011]. The performance measure is computed over 100 simulations of 20 secs each with a sampling period $\tau = T_0(\lambda) = 0.05$; the initial condition $x(0)$ for each simulation is randomly picked from an interval $[-3, 3]$. The primary focus here is to evaluate the ETMs, so ETMs in Wang et al. [2016] and Postoyan et al. [2011] are adapted so as to fit the specific example in (31). From Table 1 it can be inferred that a dynamic periodic event-triggered controller can perform better than a static periodic event-triggered controller (namely, Wang et al. [2016]) and a continuous-time event-triggered controller (namely, Postoyan et al. [2011]) for nonlinear plants.

Subsequently, to make a comparison amongst the two methods discussed in this paper, we first remove the effect of gain γ. This is done by adopting Lyapunov functions and related quantities of M.II to M.I as mod. M.I ($\sigma \neq 0$)
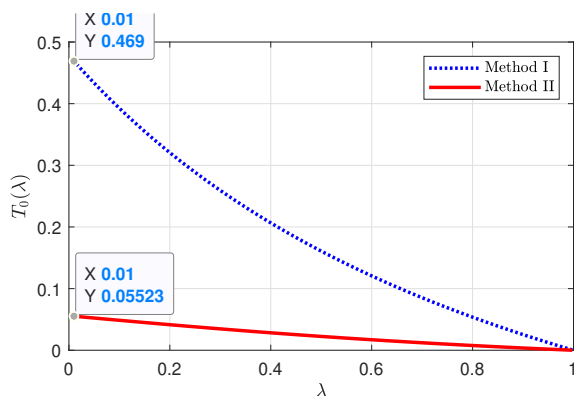
(a) MASP i.e. $T_0(\lambda)$ as a function of parameter λ
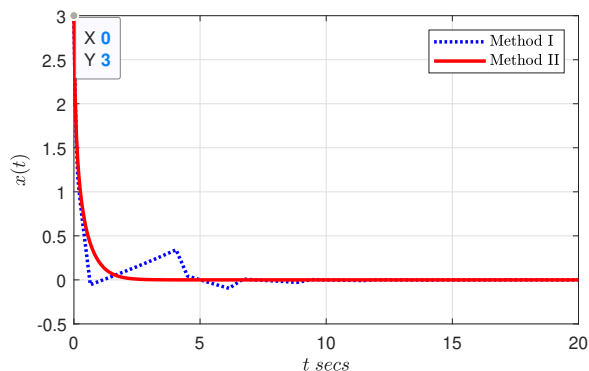
(b) Convergence of state trajectories

Fig. 2. Plots depicting MASP curves and state trajectories of Method I and Method II.

M.I	M.I ($\sigma = 0$)	Wang et al. [2016]	Postoyan et al. [2011]
14.9	13.0	66.52	15.79

Table 1. Average no. of triggers over 100 simulations in 20 secs

M.II	mod. M.I ($\sigma \neq 0$)	mod. M.I ($\sigma = 0$)
360.58	343.04	348.22

Table 2. Average no. of triggers over 100 simulations in 20 secs

and mod. M.I ($\sigma = 0$). Table 2 provides performance comparison of the ETMs of the two methods.

6. CONCLUSIONS

We proposed two methods to design dynamic periodic ETM for nonlinear systems using state feedback and provide an upper bound on the sampling period that is dependent on a user defined parameter. For each of the methods, the design results in a closed-loop hybrid system which is asymptotically stable. Since the dynamic ETM is evaluated only at event-verifying (sampling) instants, the scheme is easily implementable on digital platforms compared to its continuous-time counterparts. A comparative study on illustrative example supports the view that a dynamic ETC is capable of reducing the number of events triggered compared to its static counterparts. Finally, to the best of our knowledge, this is the first work in literature to study dynamic periodic ETC for nonlinear systems.

REFERENCES

D. P. Borgers, V. S. Dolk, and W. P. M. H. Heemels. Dynamic event-triggered control with time regularization for linear systems. In *2016 IEEE 55th Conference on Decision and Control (CDC)*, pages 1352–1357, 2016.

D. P. Borgers, V. S. Dolk, and W. P. M. H. Heemels. Dynamic periodic event-triggered control for linear systems. In *Proceedings of the 20th International Conference on Hybrid Systems: Computation and Control*, HSCC '17, 2017.

F. H. Clarke. *Optimization and Nonsmooth Analysis*. New York: Inter-science, 1983.

V. S. Dolk, D. P. Borgers, and W. P. M. H. Heemels. Output-based and decentralized dynamic event-triggered control with guaranteed $\mathcal{L}_p$- gain performance and zeno-freeness. *IEEE Transactions on Automatic Control*, 62(1):34–49, 2017.

A. Girard. Dynamic triggering mechanisms for event-triggered control. *IEEE Transactions on Automatic Control*, 60(7):1992–1997, 2015.

R. Goebel, R. G. Sanfelice, and A. R. Teel. *Hybrid Dynamical Systems: Modeling, Stability, and Robustness*. 2012.

W. P. M. H. Heemels, M. C. F. Donkers, and A. R. Teel. Periodic event-triggered control for linear systems. *IEEE Transactions on Automatic Control*, 58(4):847–861, 2013.

W. P. M. H. Heemels, R. Postoyan, M. C. F. Donkers, A. R. Teel, A. Anta, P. Tabuada, and D. Nesic. *Periodic event-triggered control*, pages 105–119. Embedded systems. CRC Press, 1 2015.

D. Liberzon, D. Nesic, and A. R. Teel. Lyapunov-based small-gain theorems for hybrid systems. *IEEE Transactions on Automatic Control*, 59(6):1395–1410, 2014.

M. Mazo, A. Anta, and P. Tabuada. An ISS self-triggered implementation of linear controllers. *Automatica*, 46(8): 1310 – 1314, 2010.

D. Nesic, A. R. Teel, and D. Carnevale. Explicit computation of the sampling period in emulation of controllers for nonlinear sampled-data systems. *IEEE Transactions on Automatic Control*, 54(3):619–624, 2009.

R. Postoyan, A. Anta, D. Nešić, and P. Tabuada. A unifying lyapunov-based framework for the event-triggered control of nonlinear systems. In *2011 50th IEEE Conference on Decision and Control and European Control Conference*, pages 2559–2564, 2011.

R. Postoyan, A. Anta, W. P. M. H. Heemels, P. Tabuada, and D. Nešić. Periodic event-triggered control for nonlinear systems. In *52nd IEEE Conference on Decision and Control*, pages 7397–7402, 2013.

L. Praly and Y. Wang. Stabilization in spite of matched unmodeled dynamics and an equivalent definition of input-to-state stability. *Mathematics of Control, Signals and Systems*, 9(1):1 – 33, 1996.

W. Wang, R. Postoyan, D. Nešić, and W. P. M. H. Heemels. Stabilization of nonlinear systems using state-feedback periodic event-triggered controllers. In *2016 IEEE 55th Conference on Decision and Control (CDC)*, pages 6808–6813, 2016.

H. Yu, F. Hao, and T. Chen. A uniform analysis on input-to-state stability of decentralized event-triggered control systems. *IEEE Transactions on Automatic Control*, 64 (8):3423–3430, 2019.